Journal of Mining and Environment (JME), Vol. 14, No. 3, 2023, 981-997

Shahrood University of Technology

Journal of Mining and Environment (JME)

Journal homepage: www.jme.shahroodut.ac.ir

Iranian Society of Mining Engineering (IRSME)

Application of Fuzzy Gamma Operator for Mineral Prospectivity Mapping, Case Study: Sonajil Area

Samaneh Barak[1], Ali Imamalipour[1*], and Maysam Abedi[2]

1. Department of Mining Engineering, Faculty of Engineering, Urmia University, Urmia, Iran
2. School of Mining Engineering, College of Engineering, University of Tehran, Tehran, Iran

Article Info

Received 18 April 2023
Received in Revised form 13 June 2023
Accepted 23 June 2023
Published online 23 June 2023

DOI:10.22044/jme.2023.12954.2352

Keywords

Mineral prospectivity mapping (MPM)
Fuzzy gamma operator
Cu-Au porphyry
Integration
Sonajil

Abstract

The Sonajil area is located in the east Azerbaijan province of Iran. According to studies on the geological structure, the region has experienced intrusive, subvolcanic, and extrusive magmatic activities, as well as subduction processes. As a result, the region is recognized for its high potential for mineralization, particularly for Cu-Au porphyry types. The main objective of this research work is to utilize the fuzzy gamma operator integration approach to identify the areas with high potential for porphyry deposits. To carry out this exploratory approach, it is necessary to investigate several indicator layers including geological, remote sensing, geochemical, and geo-physical data. The analysis reveals that the northeastern and southwestern parts of the Sonajil region exhibit a greater potential for porphyry deposits. The accuracy of the resulting Mineral Potential Map (MPM) in the Sonajil region was evaluated based on data from 20 drilled boreholes, which showed an agreement percentage of 83.33%. Due to the high level of agreement, certain locations identified in the generated MPM were recommended for further exploration studies and drilling.

1. Introduction

The exploration process comprises multiple stages that begin at a small scale and gradually expand to larger scales, ultimately leading to the identification of drilling locations that entail high costs and risks. The probability of successful exploration increases when geologists and engineers employ a comprehensive plan that encompasses different stages of exploration [1-9].

Common techniques used in mineral potential mapping within the ArcGIS environment or other software are closely associated with their conceptual models, allowing for flexibility in their application to various types of mineral deposits [8, 10].McCuaig *et al*. (2010) presented a realistic exhibition of the technique of the system to carry out exploratory goals [11]. With consideration of the common MPM (Mineral prospectivity map) application projects, the harness of restrictions in exploratory data investigation can be recognized [8, 12]. Geologists propose valuable approaches to adapt the MPM technique to address the challenges posed by imperfect real-world exploration data [10]. They suggest dividing mineral deposits into multiple studyable criteria, assessing the occurrence possibility of each criterion individually, and ultimately integrating them for the best possible outcome.

Hence, exploration experts strive to leverage all available data, maps, and the capabilities of Geographic Information Systems (GIS). Various integration methods have been proposed by different researchers to combine exploratory indicator layers and generate a Mineral Potential Map as part of the multi-criteria decision-making (MCDM) approach [12-19]. The MPM utilizes factor maps that encompass the factors influencing mineralization. This technique involves employing different methods to combine fuzzy maps using

✉ *Corresponding author: a.imamalipour@urmia.ac.ir (A. Imamalipour)*

operators such as AND, OR, PRODUCT, SUM, GAMMA, and others, either directly or through inference networks [15, 16, 20].

Two main groups, namely knowledge-driven and data-driven approaches, have been proposed for MPM to identify highly prospective areas for exploring specific ore deposits [21, 22]. In these approaches, the allocation of weights to evidential layers is based on the judgments of decision makers (DMs) [14, 15, 16, 23].

In the data-driven approach, mineral deposits under investigation are used as "training points" to capture spatial relationships within mineral geo-data sets including geology, alterations, geochemistry, and geophysics. The interactions between the input data and training data are utilized to determine the importance of each layer, which are then combined to generate a unified Mineral Potential Map (MPM). On the other hand, knowledge-driven approaches involve incorporating prior studies of the target area and the insights provided by expert geologists [21, 22].

According to the evidence such as remote sensing studies conducted on the Sonajil area by [24], the existence of Cu-Au porphyry deposit in the NE and NW parts was confirmed. By considering the available data gamma fuzzy function was employed for generating MPM in the Sonajil area [25], and the results were approved via field observation, surface sampling, and drilling.

The objective of this research work is to utilize the fuzzy gamma operator in the Sonajil area, as a knowledge-driven method, to integrate various data sets and generate MPM using ArcGIS 10.8 software for depicting more accurate results in the smaller areas. The data sets used in this study include geological layers (a combination of fault and rock units), remote sensing (alteration), geophysics (return to pole), and geo-chemistry (a combination of two layers indicating copper and gold anomalies). Each layer was assigned weights based on the conceptual model of porphyry deposits [15, 16]. The accuracy of the final MPM was assessed through 20 drilled boreholes in the area, and eventually, 83.33% agreement percentage was achieved.

2. Geological setting of Sonajil area

The Sonajil area is situated in the central part of the forest village of Haris city, located at the geographical coordinates of 38° 11' 51" north latitude and 47° 17' 14" east longitude. It is positioned approximately 17 kilometers away from Heris and directly 36 kilometers from Ahar city. Moreover, the Sonajil area is situated in the northeastern region of the 1:100,000 geological map of Ahar.

The Sonajil porphyry deposit lies in an area of widespread Cenozoic volcanic, sub-volcanic and plutonic rocks at the southeast corner of Alborz-Azerbaijan magmatic-metallogenic zone, which also are known as Aahar-Jolfa (Arasbaran) metallogenic zone. The geodynamic evolution of this belt that begun with Jurassic-Cretaceous compressive tectono-magmatism was followed by the post-collisional, extensional Neogene tectono-magmatism.

The Ahar-Jolfa zone is one of the richest Tertiary metallogenic zones of Iran. Mineralization of copper, molybdenum, gold, silver, iron, lead-zince, arsenic, antimony, and mercury has resulted in porphyry, skarn and epithermal vein deposits [19]. There are more than 10 known porphyry copper deposits and prospects this metallogenic zone including the Sungun, Masjed Daghi, Haft Cheshmeh, Saheb Divan, Sonajil, Niaz, Miveh Rud, Kighal, and Ali Javad deposits and other prospects [27].

Based on [28], the spatial distribution of the ore deposits follows three metallogenic sub-zones including (A) Ghareh Dagh, (B) Meshkin Shahr-Siahrud and (C) Sabalan-Kiamaki. The Sonajil and Mirkuh-e-Ali Mirza Cu-Au deposits lie in the eastern part of the sub-zone (C) are synchronous with Mivehrud hydrothermal system [30], which related to the Upper Miocene adakitic magmatic events [31].

Based on the geological structure of the region and the presence of a subduction zone, along with the occurrence of magmatic activities such as intrusive, subvolcanic, and particularly extrusive activities along the subduction zone, it is evident that the Sonajil area holds significant potential for mineralization, especially in relation to copper-porphyry types. The extensive magmatism activities, both in terms of temporal and spatial distribution, as well as the variation of rocks at different depths, including intrusive, subvolcanic, and extrusive rocks, further enhance the prospects of mineralization in the area. Additionally, this prospect increases more with the alteration development in the region [32, 33].

The outcrops of the Sonajil are mainly composed of Cenozoic deposits. The rock outcrops in the area can be divided into; (1) Eocene volcanic rocks: (a) Andesite unit, which seems to be the oldest lithologic unit of the area, is vastly observed in south and northwest portions. From a microscopic point of view, this unit has a porphyry texture. (b) -

- Apophyses and dykes with dioritic- granodioritic and even diabasic composition are intruded into this unit. (c)- Mega-porphyry andesite unit and porphyry andesite, (2) Oligo-Miocene intrusive masses: granitoid unit 3) Quaternary volcanic rocks: Basalt unit of quaternary, this unit is the youngest unit present in the area. A general geological map of the region is shown in Figure 1a

The volcanic-sedimentary rocks of the Eocene have spread widely in the area, and they have included about 50% of the rock outcrops in the Sonajil region. These rocks are exposed in the area's northern, eastern, and southern parts, including a massive sequence of volcano-sedimentary rocks left in the marine and continental environment [32, 33].

The most crucial alteration phases in the area include Potassic alteration, Argillic alteration, phyllic, Carbonization, and silicic alteration

Two characteristics are visible within the intrusive northern bodies of the area. The bodies that intruded into the upper members of volcanic and volcano-clastic rocks (related to the Eocene period) exhibit no extensive hydrothermal alteration halo. However, the bodies that intruded into older units and possess suitable lithologic cover display a vast alteration halo. These bodies have a higher potential for the formation of Cu-Mo and/or copper-porphyry gold deposits.

In this manner, mineralized veins are directed in E-SE, W-NW, and NW-SW strikes, while faults and fractures are directed in E-SE and W-NW strikes. Dykes with Monzodiorite composition and NE-SW trend have intercepted the altered intrusive bodies. Some silicic veins intruded into the alteration zone, parallel to mineralized veins.

3. Geological investigation

The Sonajil region is acknowledged as a promising area for porphyry Cu deposits. According to [34], host rocks and faults are two crucial factors in porphyry deposit exploration and play vital roles in determining the precise location of mineralization. The conceptual model of porphyry copper deposits was utilized to assign suitable weights for generating the rock unit indicator layer in the Sonajil area. In accordance with [34], granitoid units such as quartz monzonite, granite, and granodiorite received the highest scores, while basaltic lava flows/young alluvium, old/young terraces, and river sediments received the lowest scores. This information is presented in Table 1 and depicted in Figure 1b. The classes were fuzzified using the large membership embedded in ArcGIS 10.8. In the subsequent analysis, the buffering of faults was taken into consideration to assign weights and fuzzify the data. The areas in close proximity to faults were identified as the most influential regions and received the highest weights (as shown in Table 1 and Figure 1c). Subsequently, two indicator layers were created, one representing faults and the other representing rock units. These layers were then integrated using the weighted overlay option in ArcGIS 10.8, with 70% influence attributed to rock units and 30% influence attributed to region faults. The final geological map (Figure 1d) was generated based on this integration.

A weight of 30% was assigned to the region faults. Ultimately, the final geological map (Figure 1d) was generated.

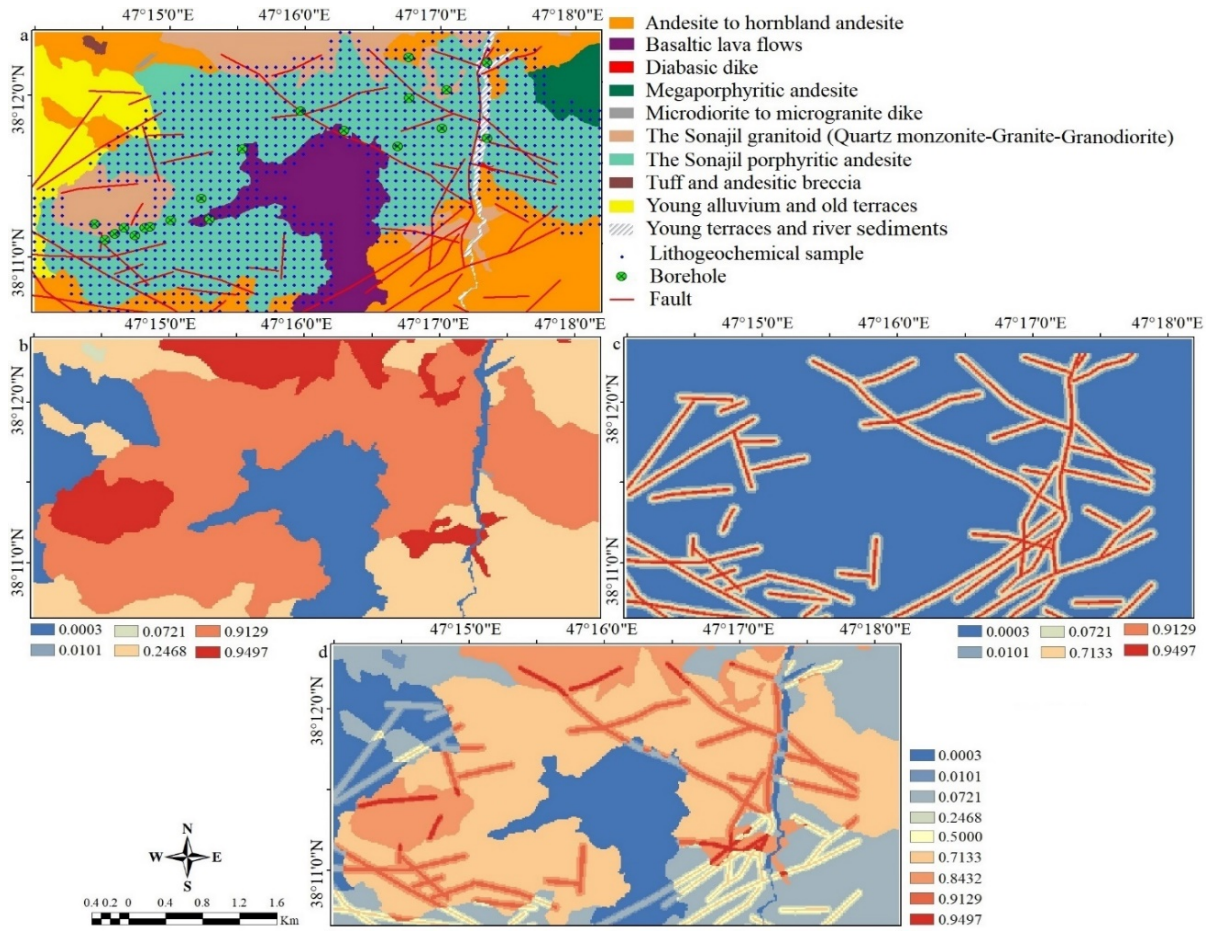

Figure 1. Detailed geological map of the Sonajil with a scale of 1:10,000 [32], rock units' evidential layer (b), faults evidential layer (c), the final geological map (d).

4. Geochemical investigation

Litho data were utilized to investigate and study the geo-chemical behavior of the Sonajil area. A total of 1248 samples were collected by [32]. The data underwent analysis for 44 elements, for 43 of them the ICP-Mass machine was used, while the F.A. machine was used for Au analysis. Censored values in the dataset were handled by applying the ¾ method, which replaces them based on the measurement limits provided by the laboratory. Descriptive statistics for 16 trace elements associated with copper porphyry deposits (Ag, Au, As, Bi, Cu, K, Mn, Mo, Pb, Rb, Re, Sb, Sn, Te, W, and Zn) are summarized in Table 2. Statistical charts including histograms, boxplots, and q-q plots for Cu are displayed in their non-normalized form in Figure 2. After adjusting the outlier values, the data was normalized. The set of 44 elements underwent factor and cluster analysis as part of the multivariate statistical processing.

Regarding the factorial analysis [35], the components were determined, the factor loadings after rotation was examined for the first 7 factors. Table 3 presents the analysis after rotation, yielding the following results:

The first component shows that elements (Be, K, Rb), (Th, U), and (Ba, W) have a strong positive loading (> 0.6), while Cr and Sr exhibit a significant negative loading. This factor indicates potassium-enriched zones and the abundance of common elements in economic mineralization. It also suggests the presence of felsic rocks as a predominant rock type.

The second component reveals that elements (Ce, La), Nb, and P display a significant positive loading. This component also points to another type of rocks, primarily consisting of felsic rocks in the region. These elements indicate late magmatic alkaline phases.

In the third component, the elements Bi, As, Mo, S, and Te exhibit a strong positive loading, while Ca and Na, which are prominent elements in plagioclase feldspars, show a significant negative loading. This suggests that mineralization

throughout the Sonajil area is characterized by an increase in the four variables of S, Te, Bi, Mo, and As, as well as a decrease in the Ca and Na elements. Consequently, this component can help identify areas that are more favorable for mineralization.

The fourth component highlights the significance of elements Co, Fe, Mn, Sc, and V, which are associated with rock-forming components (alkaline rocks). However, this component may not be crucial for exploring high-potential areas and mineralization in the Sonajil region.

Table 1. Assigned weights to the factor layers in Kahang area.

Layer	Class	Assigned weight
Rock units	Andesite to hornbland andesite	4
	Basaltic lava flows	1
	Diabasic dike	2
	Megaporphyritic andesite	4
	Microdiorite to microgranite dike	4
	The Sonajil granitoid (Quartz monzonite-Granite-Granodiorite)	9
	The Sonajil porphyritic andesite	8
	Tuff and andesitic breccia	3
	Young alluvium and old terraces	1
	Young terraces and river sediments	1
Faults (40 meters buffering)		
	5 meters	9
	10 meters	8
	20 meters	6
	30 meters	3
	40 meters	2
	background	1
Geo-chemistry		
Cu	Probable anomaly	9
	Possible anomaly	8
	Threshold	4
	Background	1
Au	Probable anomaly	8
	Possible anomaly	6
	Threshold	3
	Background	1
Alternation		
	Potassic	9
	Phyllic	8
	Argillic	7
	Propylitic	3
	background	1
Geo-physics		
	High	9
	Medium	7
	Low	4
	Very low	2
	background	1

In the fifth component, the elements Au, Cd, Re, and Sb demonstrate a relatively significant loading. These elements are typically associated with super-mineral and epithermal mineralization. This factor may indicate the upper parts of porphyry mineralization.

The sixth component shows the individual occurrence of the Hg element with a high loading, indicating the extensive erosion in this particular part. The seventh factor exhibits the highest factor loading for the Cu and Zn elements. Consequently, this factor can be regarded as a crucial indicator for copper mineralization.

The dendrogram generated from cluster analysis (Figure 3) reinforces the findings obtained from the factorial analysis, with some slight variations. The first branch of the dendrogram corresponds to the first and second factors. Within this branch, the elements Nb, La, and Ce form one group, while the elements Th, U, K, Rb, and Be comprise another group that is associated with rock formation components. Another branch of the dendrogram corresponds to the fourth factor, which includes the elements Sc, V, Fe, and Mn, indicating their relationship with petrification processes. The third factor is represented by the elements Bi, Te, As, S,

and Mo, indicating their association with molybdenum mineralization. Furthermore, this analysis confirms the strong correlation between Cu and Au among all the elements.

Based on the dendrogram data and the results of the factor analysis, the following eleven elements (As, Au, Bi, Cd, Cu, Mo, Re, S, Sb, Te, and Zn) can be considered as areas susceptible to exploring porphyry deposits in the Sonajil area.

The concentration-number (C-N) fractal method, as utilized in previous studies [36, 37, 38, 39, 40, 41], was employed to distinguish Cu and Au anomalies from the background in the Sonajil area. This fractal technique resulted in the classification of the area into four zones: background, threshold, possible (high) anomaly, and probable (very high) anomaly. Fuzzifying maps were generated to produce Cu and Au geochemical indicator layers. The assigned weights for the classified zones are presented in Table 1. Eventually, these two indicators (Figures 4a-d) were integrated using the OR operator to create the final geochemical layer (Figure 4e).

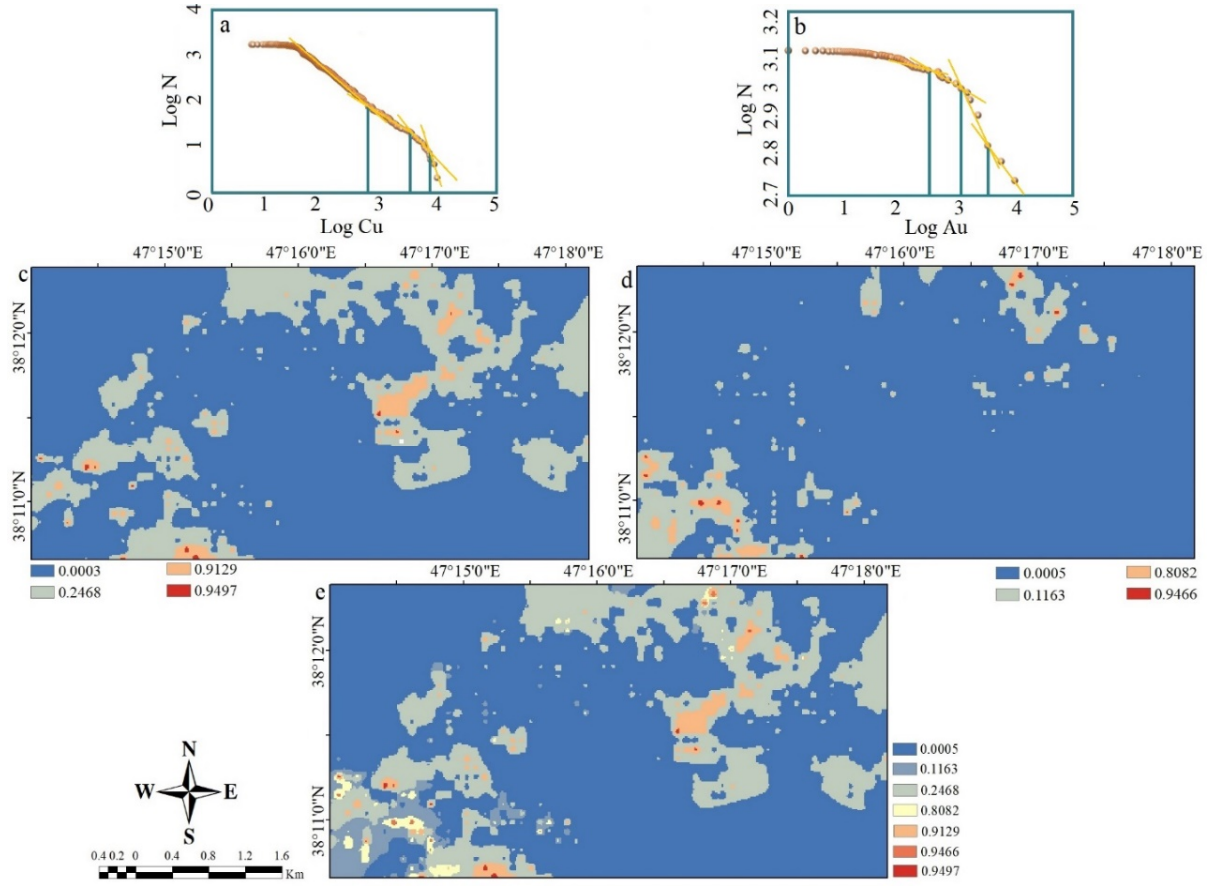

Figure 4. (a) Logarithmic diagram of concentration – number for copper, and (b) for gold, (c) the evidential map of copper and (d) gold, (e) the final geochemistry map of the Sonajil area.

Table 2. Descriptive Statistics of geo-chemical elements of Sonajil area.

	Minimum	Maximum	Mean	Std. Deviation	Skewness	Kurtosis
Ag	0.00	8890.00	24.39	283.48	26.16	781.87
As	0.00	5210.00	650.37	405.69	2.34	16.62
Au	0.00	76.00	14.31	14.45	1.34	0.72
Bi	0.80	3920.00	927.12	312.57	1.98	14.76
Cu	26.00	177000.00	23331.50	17660.31	1.20	4.86
K	0.00	349.00	113.53	52.52	0.88	0.95
Mn	0.00	47500.00	1450.30	3745.57	6.00	47.09
Mo	0.00	382.00	98.29	59.54	0.98	1.80
Pb	0.20	227.00	20.28	18.36	4.85	40.03
Rb	0.00	4.40	0.15	0.40	5.72	40.70
Re	0.20	37.80	10.96	6.40	0.38	-0.24
Sb	0.30	151.00	4.73	6.85	10.05	177.75
Sn	1.00	939.00	73.07	41.82	7.69	148.25
Te	0.30	25.40	3.31	2.72	2.46	9.91
W	0.40	285.00	64.27	48.88	1.12	1.18
Zn	0.61	26.50	10.80	4.49	0.31	0.18

5. Alteration investigation

Alteration zones are formed as a result of hydrothermal fluid interaction with geological units and exhibit distinct characteristics compared to their surroundings. These zones typically surround the core, which is the productive intrusive mass, and can be identified using specific patterns. Porphyry copper deposits are often associated with alteration zones such as potassic, phyllic, argillic, and propylitic. In porphyry mineralization, a quartz core and potassium minerals are surrounded by clay minerals and other hydroxyls that exhibit unique absorption characteristics in visible and near-infrared wavelengths [34, 42]. Detecting these alteration zones is crucial for successful exploration of the deposit. This technique offers advantages over other exploration methods due to its lower cost and ability to cover a larger area. Remote sensing methods, including the use of the ASTER (Advanced Spaceborne Thermal Emission and Reflection Radiometer) satellite sensor on the TERRA platform, have proven to be critical for identifying alterations [12, 15, 16]. Prior to data processing and analysis in the remote sensing environment, operational steps, known as pre-processing, are applied to ensure the data is suitable and useful. Typically, image pre-processing involves radiometric correction, geometric correction, atmospheric correction, and cropping the image to the desired area [43]. In the case of the Sonajil studied area, all these pre-processing steps were conducted on the ASTER image using the ENVI 4.8 (Environment for Visualizing Images) software. Both image-based and spectrum-based techniques were applied to analyze the Sonajil ASTER image.

3.2. Image-based processing methods and analysis

Image analysis involves the discrete and selective selective recognition of phenomena based on their spectral reflection in various wavelengths. Statistical techniques such as band rationing, principal component analysis (PCA), and false color composite (RGB) are commonly employed for this purpose. Different color and grayscale images can identify various phenomena through these methods, considering factors such as color, texture, shape, topography, waterway patterns, geological location, and more. In this study, band rationing is utilized as the image-based technique, as it enables the identification of minerals based on their unique absorption and reflection features in different wavelength bands. By applying band ratios that depict absorption and reflection, an output image representing the targeted mineral can be generated. The ASTER satellite images' VNIR and SWIR bands are combined in various permutations to create different band ratio combinations [12, 15, 16]. In this study, this technique is applied to the ASTER image of the Sonajil region to detect phyllic, argillic, and propylitic alterations, as shown in Figures 5a, 5b, and 5c, respectively. Furthermore, based on the spatial distribution of silicate and carbonate minerals in the thermal bands (8-12 micrometers); as presented by [44], the presence of quartz, which exhibits absorption in the 10 and 12 bands and reflection in the 11 band, can be indicative of the potassic alteration zone. Therefore, by using the

inverse of the Qi ratio, the potassic alteration in porphyry deposits can be detected [45], as shown in Figure 5d.

3.3. Spectrum-based image processing methods and analysis

To implement this approach, a spectral reference or spectral curve is necessary. In this procedure, the software compares the characteristics of the target spectrum with the satellite data set, identifies the target spectra, and extracts them. In the case of detecting porphyry copper alterations, spectral analysis can be applied to the minerals listed in Table 4. Moreover, each spectral signature can be extracted from the Spectral Library within the Envi 4.8 software.

Table 3. Rotated matrix of the factor analysis in the Sonajil area.

	Component						
	1	**2**	**3**	**4**	**5**	**6**	**7**
Ag	0.128	0.378	-0.211	-0.117	0.201	0.406	0.013
Al	0.259	0.398	0.241	0.339	-0.385	-0.165	-0.203
As	0.207	-0.542	0.554	-0.008	0.307	0.081	-0.090
Au	0.o75	-0.156	0.062	-0.059	0.671	-0.133	0.234
Ba	0.672	0.008	-0.025	0.024	-0.047	-0.207	-0.009
Be	0.800	0.137	-0.074	-0.081	0.023	0.036	0.127
Bi	0.038	-0.123	0.678	0.062	0.010	-0.152	0.214
Ca	-0.393	0.336	-0.583	0.414	-0.009	-0.088	0.067
Cd	0.176	-0.012	-0.089	-0.112	0.634	0.224	0.207
Ce	0.170	0.897	-0.096	-0.035	-0.028	0.050	-0.004
Co	-0249	0.193	-0.397	0.730	-0.048	-0.113	0.21l6
Cr	-0.621	0.445	0.038	0.194	-0.105	-0.121	0.183
Cs	0.407	-0.346	-0.079	0.172	0.102	-0.181	0.118
Cu	0.123	-0.160	0.095	0.223	0.334	0.067	0.565
Fe	-0.1es	-0.110	0.067	0.805	-0.061	-0.014	0.148
Hg	0.073	-0.016	0.094	0.183	-0.045	0.772	-0.037
K	0.866	0.033	-0.156	-0.225	0.001	0.090	0.058
La	0.165	0.918	-0.114	-0.021	-0.037	-0.004	-0.072
Li	-0.135	-0.021	0.529	0.132	0.502	0.136	-0.372
Mg	-0246	0.382	-0.416	0.584	-0.152	-0.258	0.105
Mn	0.106	-0.124	-0.511	0.609	0.118	0.052	0.085
Mo	0.219	-0.078	0.627	-0.213	0.365	0.205	0.195
Na	-0.101	0249	-0.669	0.169	-0.440	-0.175	0.200
Nb	0.343	0.619	-0.21l6	-0.219	-0.197	0.369	0.042
Ni	-0.484	0.558	-0.247	0.174	-0.028	-0.218	0.227
P	-0.317	0.623	-0.075	0.387	-0.353	0.090	0.081
Pb	0.167	0.104	0.526	-0.364	-0.030	0.040	0.337
Rb	0.888	0.051	-0.023	-0.176	0.114	0.127	0.042
Re	0.381	0.100	0.172	0.103	0.589	-0.178	-0.057
S	-0258	-0.006	0.745	0.016	-0.027	-0.082	-0.175
Sb	0.302	-0.411	0.305	-0.223	0.593	-0.025	-0.072
Sc	-0.066	0.128	-0.030	0.860	-0.048	0.083	-0.026
Sn	0.571	0.106	0.181	-0.096	0.138	0.457	0.225
Sr	-0.611	0.393	0.060	0.283	-0.324	-0.045	-o.1n
Te	-0.171	-0.161	0.760	0.047	-0.011	0.004	-0.124
Th	0.727	0.479	0.081	-0.082	0.193	0.233	-0.109
Ti	-0.311	0.467	-0.185	0.566	-0.398	0.018	0.076
Tl	0.631	-0.270	0.251	-0.131	0234	-0.211	0.287
U	0.765	0204	0.162	-0.167	0.162	0.279	-0.162
V	-0.152	-0.235	0.192	0.848	-0.076	0.052	0.002
W	0.699	-0.126	0.133	-0.192	0.391	0.335	-0.010
Y	0.635	0.360	-0.281	0.281	0264	0.162	-0.094
Zn	-0.014	0.165	-0.269	0.361	0.139	-0.088	0.635
Zr	0.320	0.508	-0.345	-0.169	-0.136	0.500	-0.168

Table 4. Indicator minerals for the alterations of copper porphyry deposits.

Alterations	Minerals
Propylitic	Chlorite, Epidote, Calcite
Argillic	Kaolinite, Montmorillonite, Illite
Phyllic	Sericite, Quartz, Pyrite

The Spectral Information Divergence (SID) method is utilized for spectral classification by calculating the divergence between pixels and known spectra. Lower divergence values indicate a higher likelihood of pixel similarity. Pixels with a divergence measurement exceeding a specified threshold are not classified [46]. The SID method is employed to distinguish phyllic, argillic, and propylitic alterations in the Sonajil area, represented in Figures 5e, f, g.

Linear Spectral Unmixing (LSU) involves decomposing the target spectrum of a mixed pixel into its constituent spectra, known as endmembers, and creating an image fraction collection that indicates the proportion of each endmember present in the pixel. LSU operates under the assumptions that: 1) each endmember is known, 2) multiple scattering among different endmembers is negligible, 3) endmembers have sufficiently distinct spectral characteristics to allow separation, and 4) a pixel is a linear combination of its constituent endmembers [47]. LSU is also employed to identify phyllic, argillic, and propylitic alteration zones in the Sonajil area, depicted in Figures 5h, i, j.

The Binary Encoding (B.E.) classification approach transforms the data and endmember spectra into binary values (zeros and ones). This transformation is performed based on whether a band value falls below or above the average spectrum value. An Exclusive OR (XOR) operator compares each encoded reference spectrum with the encoded data spectra and generates a classification image. All pixels are classified to the endmember with the highest number of matching bands, unless a minimum match threshold is set, in which case some pixels may remain unclassified if they do not meet the criteria [48]. B.E. is the final technique employed for detecting phyllic, argillic, and propylitic alterations in the Sonajil area, illustrated in Figures 5k, l, m.

Based on the exported maps (Figure 5a-m), a general alteration map of the Sonajil area was generated (Figure 5n). This map classifies the area into four alteration classes: potassic, phyllic, argillic, and propylitic. To create the final indicator map of alteration, fuzzification was applied, taking into account the conceptual model of porphyry deposits. Table (1) presents the assigned weights for the classified zones.

6. Geophysical investigation

In the Sonajil area, magnetometry studies were conducted to measure the intensity of the Earth's magnetic field. These studies are useful for exploring mineral resources that contain magnetite iron ore, as they provide insights into the characteristics of these resources through measurements of the total intensity of the magnetic field and analyzing the rate of change in this intensity using mathematical methods.

The surveying grid used in the Sonajil area had dimensions of 20 × 50 meters, with 20 meters for the east-west direction and 50 meters for the north-south direction. The recorded magnetic data showed a significant difference between the minimum and maximum values, amounting to approximately 2,400 nT. The Earth's magnetic field intensity in the region was measured to be around 48,920 nT.

The SCINTREX ENVI pro-Proton Magnetometer device was used to record the magnetic data. To process the data, IGRF (International Geomagnetic Reference Field) and diurnal correlations were applied using the Geosoft_Oasis montaj 6.4.2 software. This processing allowed for the creation of a total field magnetic (residual) map.

The bipolar nature of magnetic anomalies can complicate the analysis of magnetic maps, as the origin of the anomaly is typically located between the positive and negative poles. To address this issue, the "return to the pole" filter is commonly used. At the magnetic north pole of the Earth, the magnetic vector enters the Earth vertically, causing the positive pole to strengthen and align directly above its origin, while the negative pole weakens and migrates towards the edges of the anomaly. This filter helps reduce the complexity of the magnetic field intensity map, and the locations of magnetic origins coincide with the positive pole.

In the Sonajil area, the reduced-to-pole (RTP) transformation was applied to the residual magnetic data. This transformation removes the inclination effect of the induced magnetic field by relocating it to the magnetic north pole. Additionally, weights were assigned to different magnetic rate classes based on a given criteria (as shown in Table 1). Fuzzification was then applied using a Gaussian membership type to generate the final indicator geophysical (RTP) map, as depicted in Figure 6.

According to previous studies [15, 16], areas with high magnetic intensity levels are typically associated with unaltered rocks, while regions with low magnetic intensity levels are linked to regional sediments. These areas may not exhibit significant relevance to mineralization. The geophysical (RTP) map can help identify potential mineralization zones based on the locations of medium anomalies.

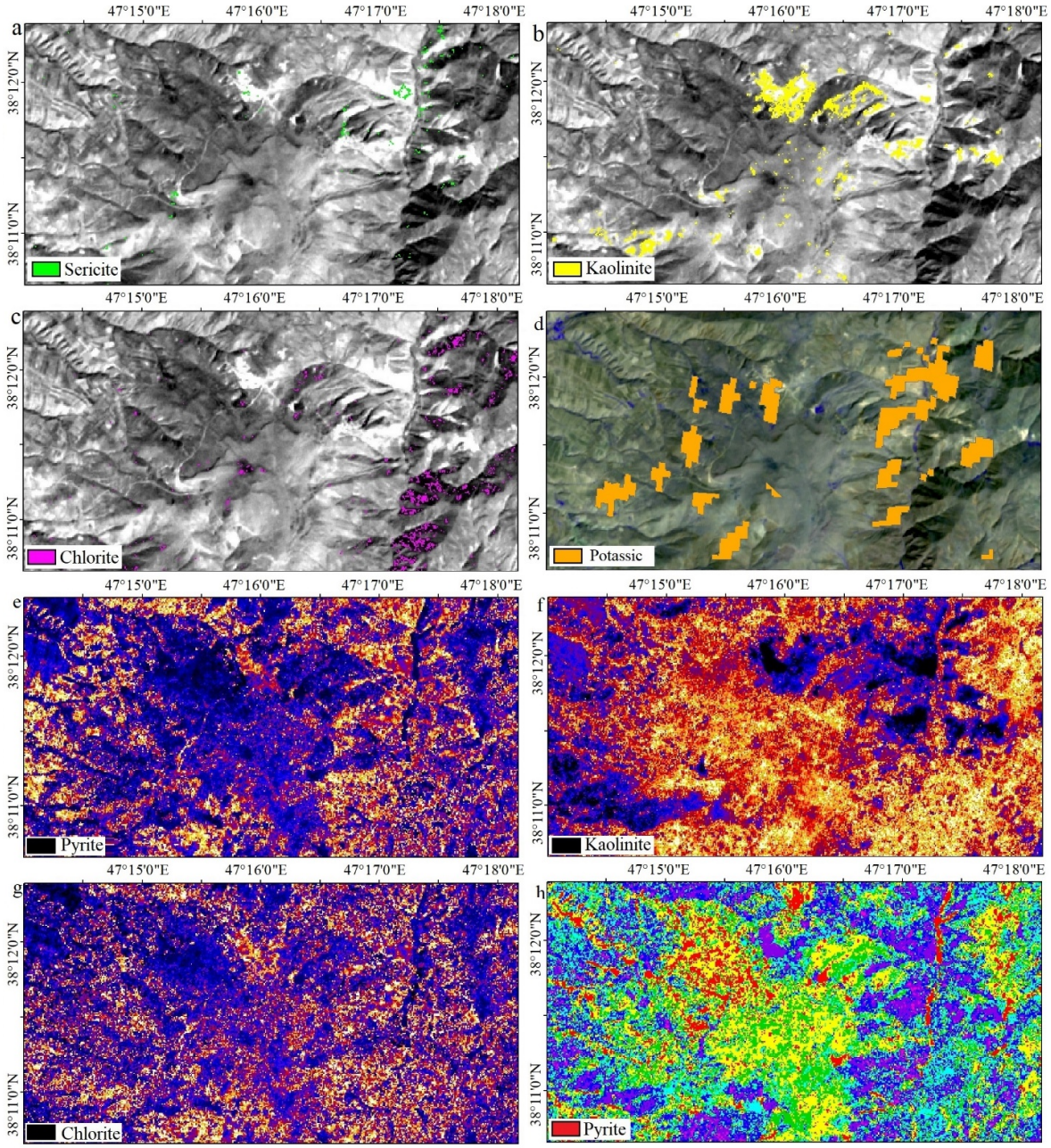

Figure 5. Output alterations of phyllic, argillic, and propylitic by using various techniques of band rationing (a) to (d), SID (e) to (g), LSU (h) to (j), BE (k) to (m), the final alteration map (n).

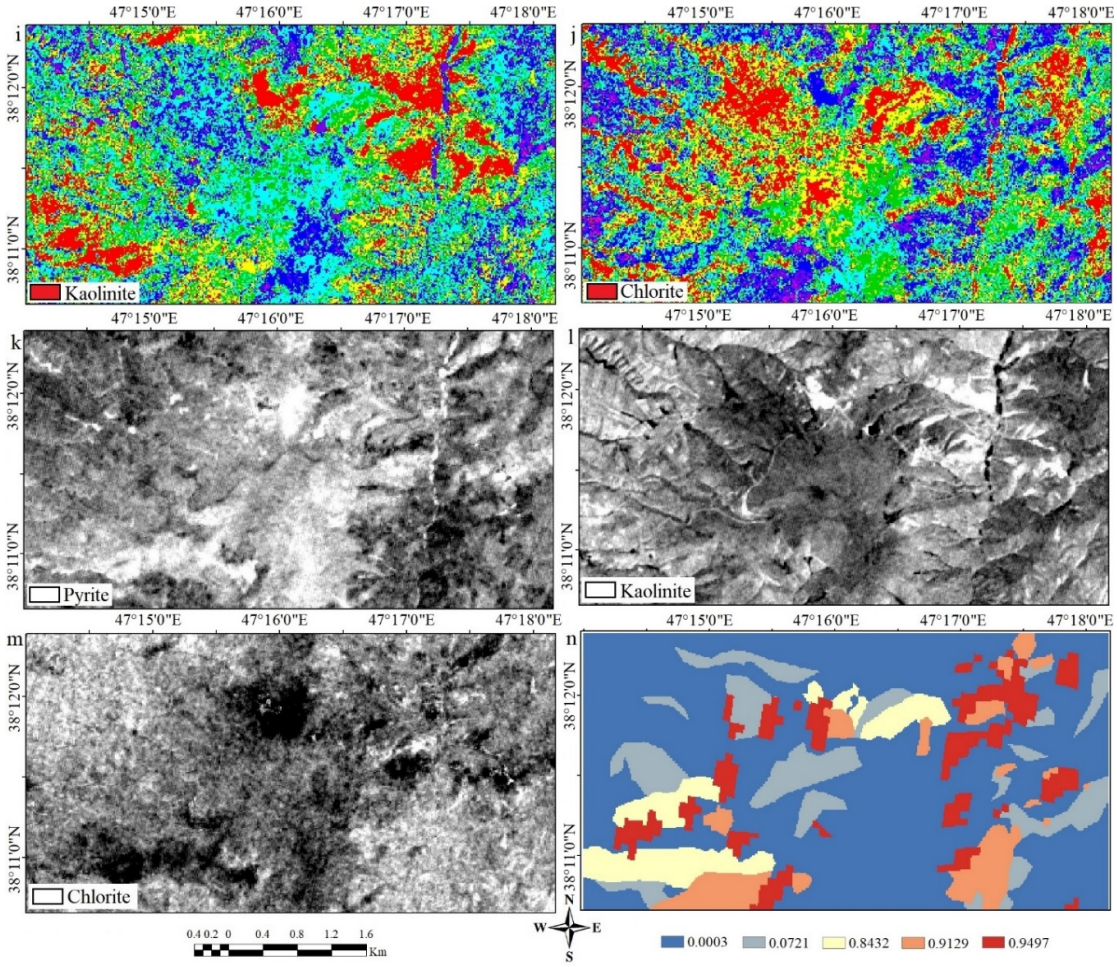

Figure 5. (continued).

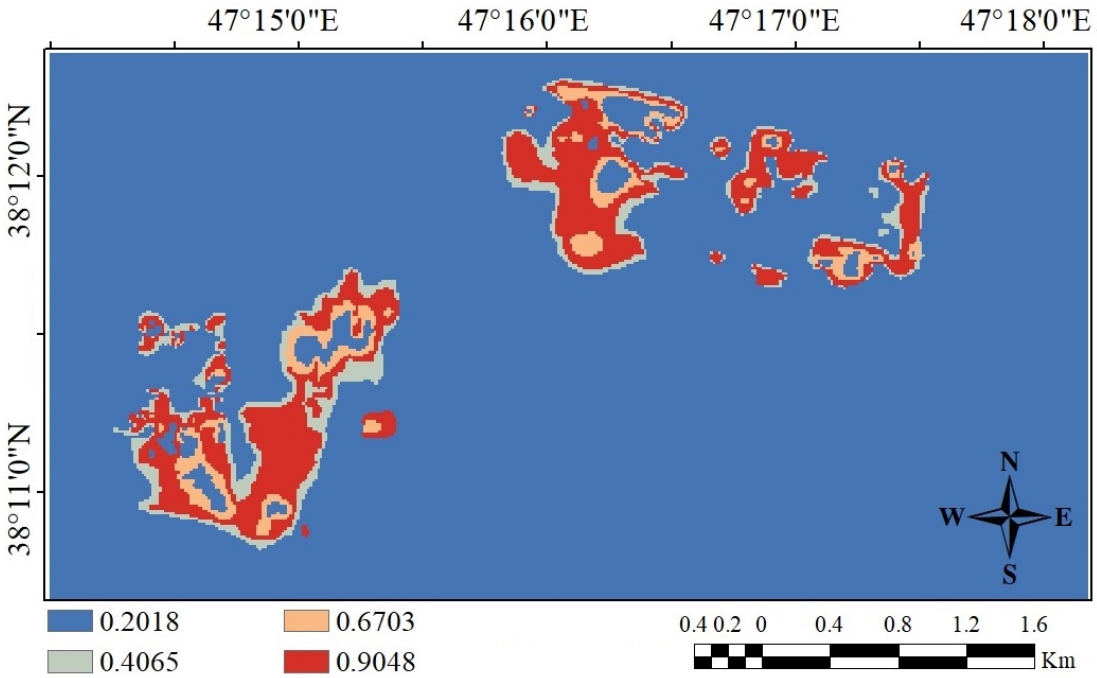

Figure 6. Geophysical magnetometery layers of the reduced to pole (RTP).

7. Layer fusion using the fuzzy gamma operator

The fuzzy set theory, introduced by [49], provides a mathematical framework for investigating natural phenomena in the environment. In this theory, a fuzzy set represents an object classified by graded sequences of membership. Membership values are assigned between 0 and 1, indicating the level of certainty or degree of belongingness of an object to a particular class or category. Fuzzy set theory allows for a more flexible representation of uncertainty and ambiguity in data analysis.

In the context of this study, fuzzy set theory is employed to integrate multiple indicator maps with fuzzy membership functions using the fuzzy gamma operator. The fuzzy gamma operator is a combination of the fuzzy algebraic product and the fuzzy algebraic sum, controlled by the gamma parameter, which ranges from 0 to 1. It provides a flexible approach for integrating weighted maps and can be easily implemented using software such as ArcGIS.

In this study, the fuzzy gamma operator is used to to fuse the fuzzy membership functions and create a mineral potential map. The selection of membership weights is determined by the geo-expert based on their expertise and understanding of the study area. The gamma value, which controls the degree of influence of each membership function, is determined through a trial-and-error approach. In the Sonajil area, the gamma value of 0.87 is chosen, and the final Mineral Potential Map (MPM) is generated, as depicted in Figure 7.

It's important to note that the selection of fuzzy membership weights and the gamma value requires expert judgment and can be tailored to the specific study area and objectives of the analysis.

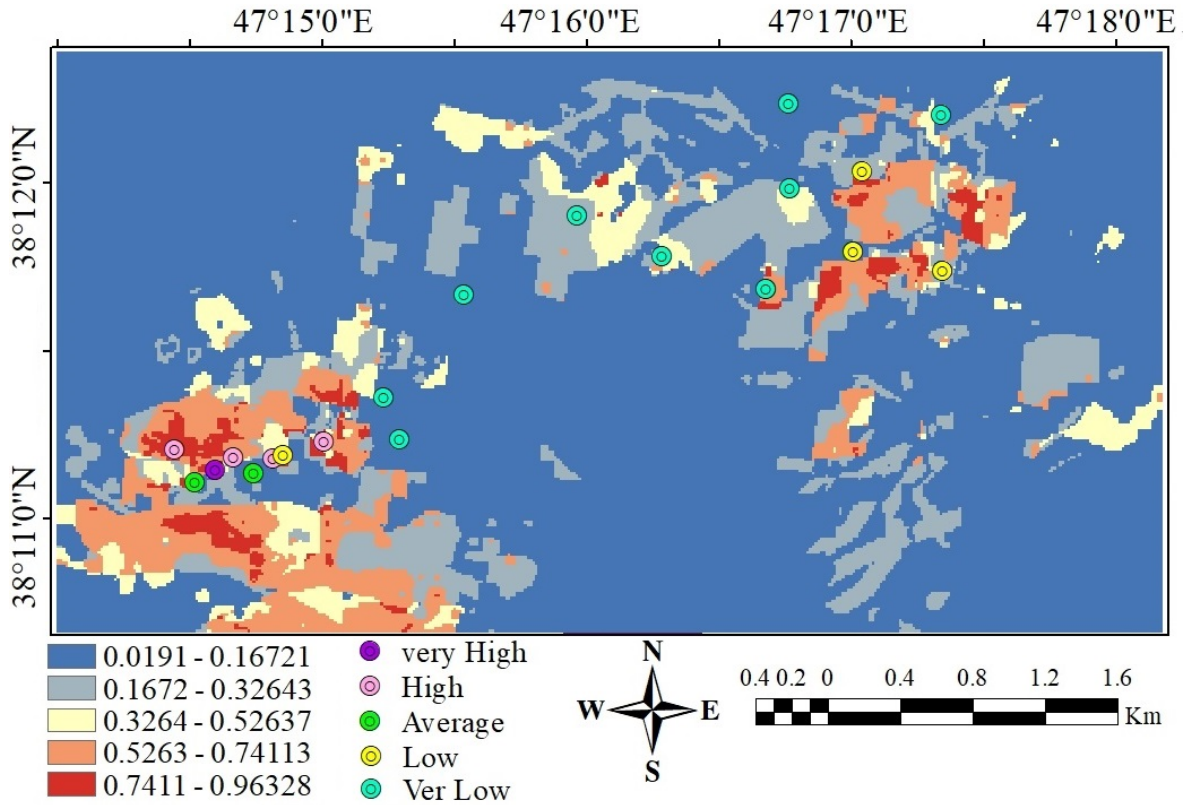

Figure 7. Final mineral prospectivity map in the Sonajil area using fuzzy gamma operator.

8. Discussions

In this study, Mineral Prospectivity Mapping (MPM) is conducted to identify potential regions for porphyry copper mineralization in the Sonajil area. The MPM approach integrates various geospatial datasets including geology, remote sensing, geochemistry, and geophysics to analyze and fuse the information and identify areas with a high likelihood of hosting economically viable mineralized targets.

The geospatial database used in this study consists of four main criteria: geology (rock units and faults), remote sensing (alteration), geochemistry (Cu and Au anomalies), and geophysics (RTP). These criteria provide valuable

information related to the presence of porphyry copper mineralization. Expert knowledge from experienced professionals in porphyry mineral exploration is also incorporated into the analysis.

Six evidential layers are generated from the geospatial database, and the fuzzy gamma operator technique is applied to combine these layers and create the final MPM. The fuzzy gamma operator approach allows for the integration of weighted maps and the incorporation of expert knowledge. The gamma value, determined through a trial-and-error approach, controls the influence of each evidential layer in the final MPM.

The Jenks's natural classification method is used to classify the MPM into different classes. This classification technique aims to minimize variance within classes while maximizing variance among classes. It provides a meaningful representation of the data and generates thematic layer maps that accurately depict patterns and trends in the potential for porphyry copper mineralization.

The selection of the Jenks's natural classification method is based on its suitability for the study area and its ability to effectively represent the data according to the literature and the author's experience in the Sonajil area.

In order to assess the accuracy of the Mineral Prospectivity Mapping (MPM) results, information from 20 drilled boreholes in the Sonajil area was used. The boreholes were classified into five categories: very low, low, average, high, and very high, based on their mineralization potential.

The MPM, which was divided into five classes using the Jenks classification approach, was compared to the borehole classification. The comparison showed that there was an 83.33% agreement between the determined classes in the MPM and the actual mineralization situation in the boreholes (Table 5). This high agreement percentage indicates the reliability and accuracy of the MPM in identifying potential mineralized areas.

Based on the analysis of the Mineral Prospectivity Mapping (MPM), it is evident that the north-east and south-west portions of the Sonajil area exhibit a higher potential for mineralization. These regions show favorable characteristics and indicators according to the MPM results.

The fuzzy gamma operators utilized in the MPM analysis have demonstrated a high agreement percentage, further supporting the reliability of the findings. As a result, the red areas identified in the MPM (as shown in Figure 7) are considered highly promising for future exploration studies and drilling activities.

Table 5. Comparison between obtained MPM and Jenk classification approach.

Borehole	Status of borehole classified to 5 groups	Status of classification to 5 groups	Score	Borehole	Status of borehole classified to 5 groups	Status of classification to 5 groups	Score
1	High	Very high	-1	12	Very low	Very low	0
2	Average	High	-1	13	Very low	Low	-1
3	Very high	Very high	0	14	Very low	Very low	0
4	High	High	0	15	Low	Low	0
5	High	Very high	-1	16	Very low	Very low	0
6	High	Very high	-1	17	Low	Low	0
7	Low	Average	-1	18	Very low	Very low	0
8	Average	Very low	2	19	Very low	Very low	0
9	Very low	Low	-1	20	Very low	Very low	0
10	Low	Very low	1				
11	Very low	Very low	0		Agreement percentage		83.33%

9. Conclusions

In conclusion, this study aimed to identify promising areas for Cu-Au porphyry mineralization in the Sonajil area. The conventional and popular fuzzy gamma operator in MPM was chosen as the integrated approach, allowing for flexible integration of weighted maps from various data sets including geology, remote sensing, geochemistry, and geophysics. Two main distinct zones, the north-east (N.E.) and south-west (S.W.) portions were highlighted as promising ore trapping regions that are closely associated to the fault mechanism of the studied area as well.

The accuracy of the map was acknowledged through previous drillings, which implies that complementary drilling can be suggested aiming at reservoir modelling. Based on the 83.33% agreement percentage, the red zones identified in the MPM were recommended as promising areas

for further exploration studies and drilling activities.

Note that a study of this kind presented here would improve our knowledge about main controllers of Cu-Au mineralization and serve as a reference for further exploration for not only in this area but also for investigating other similar areas.

Acknowledgments

This research work was made possible with the help of the office of the vice-chancellor for Research and Technology, at Urmia University. We acknowledge their support.

The exploration works were conducted by the Koomeh Mine Pars Company on the Sonajil porphyry-Cu deposit. We would like to thank the exploration department of this company, especially Mr Gholamreza Asgarizadeh, manager of the Sonajil project and Mr Jamshid Habibi, engineer of the Sonajil project for giving permission to access all data and samples analysis.

References

[1]. Carranza, E.J.M. and Hale, M. (2001). Geologically constrained fuzzy mapping of gold mineralization potential, Baguio district, Philippines. Natural Resources Research, 10, 125-136.

[2]. Porwal, A., Carranza, E.J.M., and Hale, M. (2003). Knowledge-driven and data-driven fuzzy models for predictive mineral potential mapping. Natural Resources Research, 12(1): 1-25.

[3]. Yousefi, M. and Carranza, E.J.M. (2015). Fuzzification of continuous-value spatial evidence for mineral prospectivity mapping. Computers & Geosciences, 74, 97-109.

[4]. Yousefi, M. and Carranza, E.J.M. (2017). Union score and fuzzy logic mineral prospectivity mapping using discretized and continuous spatial evidence values. Journal of African Earth Sciences, 128, 47-60.

[5]. Abedi, M., Kashani, S.B.M., Norouzi, G.H., and Yousefi, M. (2017). A deposit scale mineral prospectivity analysis: A comparison of various knowledge-driven approaches for porphyry copper targeting in Seridune, Iran. Journal of African Earth Sciences, 128, 127-146.

[6]. Ghasemzadeh, S., Maghsoudi, A., Yousefi, M., and Mihalasky, M.J. (2019). Stream sediment geochemical data analysis for district-scale mineral exploration targeting: Measuring the performance of the spatial U-statistic and CA fractal modeling. Ore Geology Reviews, 113, 103115.

[7]. Rahimi, H., Abedi, M., Yousefi, M., Bahroudi, A., and Elyasi, G. R. (2021). Supervised mineral exploration targeting and the challenges with the selection of deposit and non-deposit sites thereof. Applied Geochemistry, 128, 104940.

[8]. Khalifani, F., Imamalipour, A., Barak., S., Abedi, M., Jozanikohan, G., and Bahroudi, A., (2023). The Application of Various Mineral Prospectivity Modelingin the Exploration of Orogenic Gold Deposit in Saqez-Sardasht. Lithology and Mineral Resources, 58(4): 367-385.

[9]. Yousefi, M. and& Hronsky, J. M. (2023). Translation of the function of hydrothermal mineralization-related focused fluid flux into a mappable exploration criterion for mineral exploration targeting. Applied Geochemistry, 105561.

[10]. Porwal, A., Das, R.D., Chaudhary, B., Gonzalez-Alvarez, I., and Kreuzer, O. (2015). Fuzzy inference systems for prospectivity modeling of mineral systems and a case-study for prospectivity mapping of surficial Uranium in Yeelirrie Area, Western Australia. Ore Geology Reviews, 71, 839-852.

[11]. McCuaig, T.C., Beresford, S., and Hronsky, J. (2010). Translating the mineral systems approach into an effective exploration targeting system. Ore Geology Reviews, 38(3): 128-138.

[12]. Barak, S., Imamalipour, A., Abedi, M., Bahroudi, A., and Khalifani, F.M. (2021). Comprehensive modeling of mineral potential mapping by integration of multiset geosciences data. Geochemistry, 81(4): 125824.

[13]. Abedi, M. and Norouzi, G.H. (2012). Integration of various geophysical data with geological and geochemical data to determine additional drilling for copper exploration. Journal of Applied Geophysics, 83, 35-45.

[14]. Abedi, M., Norouzi, G.H., and Bahroudi, A. (2012). Support vector machine for multi classification of mineral prospectivity areas. Computers & Geosciences, 46, 272-283.

[15]. Barak, S., Bahroudi, A., and Jozanikohan, G. (2018a). Exploration of Sonajil porphyry copper deposit using advanced integration of geological, remote sensing, geochemical, and magnetics data. Journal of Mining and Environment, 9(1): 19-39.

[16]. Barak, S., Bahroudi, A., and Jozanikohan, G. (2018b). The use of fuzzy inference system in the integration of copper exploration layers in Neysian. Iranian Journal of Mining Engineering, 13(38): 97-112.

[17]. Barak, S., Abedi, M., and Bahroudi, A. (2020). A knowledge-guided fuzzy inference approach for integrating geophysics, geochemistry, and geology data in a deposit-scale porphyry copper targeting, Saveh, Iran. Bollettino di Geofisica Teorica ed Applicata, 61(2).

[18]. Ghaeminejad, H., Abedi, M., Afzal, P., Zaynali, F., and Yousefi, M. (2020). A fractal-based outranking

approach for mineral prospectivity analysis. Bollettino di Geofisica Teorica e Applicata, 61(4): 555-588.

[19]. Panahi, S., Khakzad, A., and Afzal, P. (2022). Analytical hierarchical prospectivity mapping using integration of exploratory data in the Anarak region, Central Iran. Geopersia, 12(1): 53-68.

[20]. Zimmermann, H.J. (2010). Fuzzy set theory. Wiley interdisciplinary reviews: computational statistics, 2(3): 317-332.

[21]. Bonham-Carter, G.F. (1994). Geographic information systems for geoscientists-modeling with GIS. Computer methods in the geoscientists, 13, 398.

[22]. Carranza, E.J.M. (2008). Geochemical anomaly and mineral prospectivity mapping in GIS. Elsevier.

[23]. Tangestani, M.H. and Moore, F. (2003). Mapping porphyry copper potential with a fuzzy model, northern Shahr-e-Babak, Iran. Australian Journal of Earth Sciences, 50(3): 311-317.

[24]. Yazdi, Z., Rad, A.J., Aghazadeh, M., and Afzal, P. (2019). Porphyry copper prospectivity mapping using fuzzy and fractal modeling in sonajeel area, NW Iran. Bulletin of the Mineral Research and Exploration, 158(158): 235-250.

[25]. Yazdi, Z., Jafari Rad, A., Aghazadeh, M., and Afzal, P. (2018). Alteration mapping for porphyry copper exploration using ASTER and QuickBird multispectral images, Sonajeel Prospect, NW Iran. Journal of the Indian Society of Remote Sensing, 46, 1581-1593.

[26]. Dilek, Y., Imamverdiyev, N., and Altunkaynak, Ş. (2010). Geochemistry and tectonics of Cenozoic volcanism in the Lesser Caucasus (Azerbaijan) and the peri-Arabian region: collision-induced mantle dynamics and its magmatic fingerprint. International Geology Review, 52(4-6): 536-578.

[27]. Aghazadeh, M., Hou, Z., Badrzadeh, Z., and Zhou, L. (2015). Temporal–spatial distribution and tectonic setting of porphyry copper deposits in Iran: constraints from zircon U–Pb and molybdenite Re–Os geochronology. Ore geology reviews, 70, 385-406.

[28]. Jamali, H. and Mehrabi, B. (2015). Relationships between arc maturity and Cu–Mo–Au porphyry and related epithermal mineralization at the Cenozoic Arasbaran magmatic belt. Ore Geology Reviews, 65, 487-501.

[29]. Ghorbani, M. (2013). The economic geology of Iran. Mineral deposits and natural resources. Springer, 1-450.

[30]. Jamali, H., Yaghubpur, A., Mehrabi, B., Dilek, Y., Daliran, F., and Meshkani, A. (2012). Petrogenesis and tectono-magmatic setting of Meso-Cenozoic magmatism in Azerbaijan province, Northwestern Iran. Petrology–new perspectives and applications. Intech, 39-56.

[31]. Maghsoudi, A., Yazdi, M., Mehrpartou, M., Vosoughi, M., and Younesi, S. (2014). Porphyry Cu–Au mineralization in the Mirkuh Ali Mirza magmatic complex, NW Iran. Journal of Asian Earth Sciences, 79, 932-941.

[32]. KCE (Kavoshgaran Consulting Engineers), (2006), Report of lithogeochemical explorations in Sonajil region.

[33]. Hosseinzadeh, G.H., Mouayed, M., and Esfehanipour, R. (2009). Supergene processes in Sonajil porphyry copper deposit with respect to using of leached capping for estimation of supergene enrichment in porphyry copper deposits, 3(10): 85-96.

[34]. Sillitoe, R.H. (2010). Porphyry copper systems. Economic geology, 105(1): 3-41.

[35]. Barak, S., Bahroudi, A., Aslani, S., and Mohebi, A. (2016). The geochemical anomaly separation by using the soil samples of eastern of Neysian, Isfahan Province, Geochemistry, 5(1): 55–71.

[36]. Afzal, P., Jebeli, M., Pourkermani, M., and Jafari Rad, A. (2018). Correlation between rock types and Copper mineralization using fractal modeling in Kushk-e-Bahram deposit, Central Iran. Geopersia, 8(1): 131-141.

[37]. Afzal, P., Alghalandis, Y.F., Khakzad, A., Moarefvand, P., and Omran, N.R. (2011). Delineation of mineralization zones in porphyry Cu deposits by fractal concentration–volume modeling. Journal of Geochemical exploration, 108(3): 220-232.

[38]. Afzal, P., Zia Zarifi, A., and Sadeghi, B. (2013). Separation of geochemical anomalies using factor analysis and concentration-number (C.N.) fractal modeling based on stream sediments data in Esfordi 1: 100000 Sheet, Central Iran. Iranian Journal of Earth Sciences, 5(2): 100-110.

[39]. Hassanpour, S. and Afzal, P. (2013). Application of concentration–number (C–N) multifractal modeling for geochemical anomaly separation in Haftcheshmeh porphyry system, NW Iran. Arabian Journal of Geosciences, 6(3): 957-970.

[40]. Khalifani, F., Bahroudi, A., Barak, S., and Abedi, M. (2019). An integrated Fuzzy AHP-VIKOR method for gold potential mapping in Saqez prospecting zone, Iran. Earth Observation and Geomatics Engineering, 3(1): 21-33.

[41]. Ghasemzadeh, S., Maghsoudi, A., Yousefi, M., and Mihalasky, M. J. (2022). Information value-based geochemical anomaly modeling: A statistical index to generate enhanced geochemical signatures for mineral exploration targeting. Applied Geochemistry, 136, 105177.

[42]. Cannell, J., Cooke, D.R., Walshe, J.L., and Stein, H. (2005). Geology, mineralization, alteration, and structural evolution of the El Teniente porphyry Cu-Mo deposit. Economic Geology, 100(5): 979-1003.

[43]. Abrams, M.J., Brown, D., Lepley, L., and Sadowski, R. (1983). Remote sensing for porphyry copper deposits in southern Arizona. Economic Geology, 78(4): 591-604.

[44]. Tommaso, I. and Rubinstein, N. (2007). Hydrothermal alteration mapping using ASTER data in the Infiernillo porphyry deposit, Argentina. Ore Geology Reviews, 32(1-2): 275-290.

[45]. Ninomiya, Y. (2003, March). Rock type mapping with indices defined for multispectral thermal infrared ASTER data: case studies. In Remote Sensing for Environmental Monitoring, GIS Applications, and Geology II (Vol. 4886, pp. 123-132). SPIE.

[46]. Qin, J., Burks, T.F., Ritenour, M.A., and Bonn, W.G. (2009). Detection of citrus canker using hyperspectral reflectance imaging with spectral information divergence. Journal of food engineering, 93(2): 183-191.

[47]. Settle, J.J. and Drake, N. A. (1993). Linear mixing and the estimation of ground cover proportions. International Journal of Remote Sensing, 14(6): 1159-1177.

[48]. Scott, D.R. (1988). Effects of binary encoding on pattern recognition and library matching of spectral data. Chemometrics and intelligent laboratory systems, 4(1): 47-63.

[49]. Zadeh, L.A. (1965). Fuzzy sets. Information and control, 8(3): 338-353.

کاربرد عملگر گامای فازی برای تهیه نقشه پتانسیل معدنی (مطالعه موردی: منطقه سوناجیل)

سمانه برک[1]، علی امامعلی‌پور[1*] و میثم عابدی[2]

1. گروه مهندسی معدن، دانشکده فنی و مهندسی، دانشگاه ارومیه، ایران
2. دانشکده مهندسی معدن، دانشگاه تهران، ایران

ارسال 2023/04/18، پذیرش 2023/06/23

* نویسنده مسئول مکاتبات: a.imamalipour@urmia.ac.ir

چکیده:

منطقه سوناجیل در استان آذربایجان شرقی ایران قرار دارد. بر اساس مطالعات انجام شده بر روی ساختار زمین شناسی، منطقه دارای فعالیت‌های ماگمایی نفوذی، کم ژرفا و آتشفشانی و همچنین فرآیندهای فرورانش بوده است. در نتیجه، این منطقه به دلیل پتانسیل بالای آن برای کانی سازی، به ویژه برای انواع پورفیری Cu-Au شناخته شده است. هدف اصلی این کار تحقیقاتی استفاده از رویکرد تلفیقی عملگر گامای فازی برای شناسایی مناطق با پتانسیل بالا بر روی کانسار پورفیری است. برای انجام این رویکرد اکتشافی، بررسی چندین لایه شاهد از جمله داده‌های زمین‌شناسی، سنجش از دور، ژئوشیمیایی و ژئوفیزیک ضروری است. تجزیه و تحلیل‌ها حاکی از پتاسیل بالای کانسار پورفیری در بخش های شمال شرقی و جنوب غربی منطقه سوناجیل پتانسیل می‌باشد. دقت نقشه پتانسیل معدنی (MPM) حاصل در منطقه سوناجیل بر اساس داده‌های 20 گمانه حفاری شده ارزیابی شد که درصد تطابق 83.33 درصد را نشان می‌دهد. با توجه به تطابق بالای مدل بررسی شده، مکان‌های خاصی که در MPM شناسایی شده‌اند برای مطالعات اکتشافی و حفاری بیشتر توصیه می‌شوند.

کلمات کلیدی: نقشه برداری پتانسیل معدنی (MPM)، عملگر گامای فازی، پورفیری مس- طلا، تلفیق، سوناجیل.